

## Structural Behaviour Of Ultra High Strength Concrete Columns Under Biaxial Loading

Dr. Ghada D. Abd-Elhamid<sup>1</sup>, Dr. Enas A.A. Khattab<sup>2</sup>, Dr. Omnia F.H. Mahmoud<sup>3</sup>

<sup>1,2</sup>Assoc. Professor, Building Material and Quality Control, Research Institute, Housing & Building National Research Center.

<sup>3</sup>Assistant Professor, Construction Department, Faculty of Engineering, Egyptian Russian University, Cairo, Egypt

Corresponding Author: Dr. Ghada D. Abd-Elhamid

### ABSTRACT

Ultra High Strength Concrete (UHSC) is characterized by extraordinary mechanical properties (high compressive and tensile strength, large E-modulus) and has excellent durability properties regarding corrosion of concrete and reinforcement. Until the peak load the behavior is predominantly linear-elastic, large deformations at peak cannot be observed, and the reached post-peak strain is nearly zero. These facts point out the very brittle material behavior. The structural behavior of UHSC columns was investigated through an experimental program comprising applying biaxial bending on large-scale specimens. The experimental program of this study includes testing of five reinforced concrete square columns. The program was designed to clarify the effect of different eccentricity ratios ( $e/t = 0, 0.1, 0.2, 0.4$  and  $1.0$ ). The test results cover the cracking behavior and mode of failure, and load-concrete strain response. The test results were analyzed and evaluated to demonstrate the effect of eccentricity ratio on the ultimate capacity of UHSC columns subjected to biaxial bending. The results displayed that increasing the eccentricity from ( $e/t = 0$ ) to ( $e/t = 1.0$ ) resulted in significant reduction in ultimate load capacity by 95%. The design provisions for slender columns subjected to biaxial bending in the Egyptian Code for Design and Construction of Reinforced Concrete Structures ECP 203-2007 were evaluated and compared to the experimental results.

**Keywords:** UHSC, RC columns, Eccentricity, Biaxial loading.

Date Of Submission: 02-10-2018

Date Of Acceptance: 13-10-2018

### I. INTRODUCTION

Claeson, C., and Gylltoft, K.,<sup>[1]</sup> conducted a test series of 12 slender HSC columns with compression strengths of 50 to 120 N/mm<sup>2</sup>. The specimens had variable length to width ratios with square cross sections of 120 x 120 mm and 200 x 200 mm dimension. Test parameters were the concrete strength, the stirrup spacing, and the slenderness ratio of the column. The writers concluded that the failure of HSC column was brittle. While closer stirrup spacing did not increase the load capacity, it did contribute to a less brittle behavior after the maximum load had been reached. However, it was observed from the tests of HSC columns that closer stirrup spacing is required to obtain the same structural behavior as that of NSC column.

Ghoneim, M.<sup>[2]</sup> carried out a research program on the behavior and strength of eccentrically loaded slender HSC columns. He tested nine large scale HSC columns with square section in the vertical position. The investigated variables were the slenderness ratio and the ratio of

the eccentricity of the axial load to the column thickness. The heights of the tested columns reached 5250 mm. Ghoneim reported that the failure of columns was caused either by compressive crushing of concrete because of the limited deformability of HSC in compression, or by the instability of the slender column. He also found that the failure load was dependent on the load eccentricity as well as the column slenderness ratio; it was inversely proportional with both. The mode of failure of all specimens was typically flexure with concrete crushing in the compression zone.

Tarek, M. E.,<sup>[3]</sup> investigated the structural behavior of normal-strength and high-strength concrete slender columns through an experimental program comprising applying biaxial bending on large-scale specimens. The program was designed to clarify the effect of key parameters such as the concrete compressive strength, the longitudinal steel reinforcement ratio, the eccentricity and the slenderness ratio. The results displayed that increasing the eccentricity from 20 mm ( $e/t = 0.10$ ) to 140 mm ( $e/t = 0.70$ ) resulted in significant

reduction in ultimate load capacity and stiffness by 85% and 90%, respectively. The high strength concrete columns showed a clear brittle behavior compared to the normal strength concrete columns. Khattab. E et al <sup>[4]</sup>, investigated the behavior of short concrete columns manufactured from UHSC under axial loads. An evaluation is made to the major variables that affect the behavior of thirteen UHSC columns under axial loading. Variables covered in this evaluation include the longitudinal reinforcement ratio, percentage of steel fiber, stirrups ratio, concrete compressive strength and aspect ratio of the column. A theoretical prediction of the deformational behavior for the tested columns is developed. A design equation for designing short UHSC columns is presented. Failure modes of most columns were due to spalling of the concrete cover. Spalling became more prevalent as the concrete strength increases while the specimens with fiber reinforced UHSC fails in a more ductile mode. The equation adopted by the Canadian code nearly estimated the same ultimate axial load capacity of the tested specimens while the Equations used by ACI, ISO and British standards were under estimated the ultimate axial capacity for the columns.

During the last few years there has a rapid growth of interest in ultra-high strength concrete (UHSC). In order to use UHSC in different structural members, current design methodologies must be evaluated for their adequacy to be used in designing UHSC members. UHSC finds wide use in tall buildings, bridges, airports, power plants etc. The main objective of this research is to investigate the structural behavior of UHSC columns through an experimental program comprising applying biaxial bending on large-scale specimens. The test results cover the cracking behavior and mode of failure and load-concrete strain response. The test results were analyzed and evaluated to demonstrate the effect of eccentricity ratio on the structural behavior of the specimens.

## II. RESEARCH PROGRAM

Five reinforced column specimens were tested under the effect of biaxial loading. All specimens were of identical concrete dimensions. The column had a square cross section of 200x200 mm, 1600 mm clear height and 2400 mm overall height including corbel heads, while the top and bottom corbels were 400x400x400 mm dimensions. Those corbel heads were introduced to prevent premature failure. The main parameter of the study was eccentricity ratio ( $e/t = 0, 0.1, 0.2, 0.4$  and  $0.70$ ). Table 1 shows the columns configurations.

Table 1: Columns Configurations

Colu mn	H (mm.)	Section (mm.)	Rft.	e (mm.)	e/t
C1	2400	200*200	4 <del>φ</del> 16	0	0
C2				20	0.1
C3				40	0.2
C4				100	0.5
C5				200	1.0

## III. MATERIALS PROPERTIES

The materials used in this study were coarse aggregate which was local crushed dolomite from natural resources with nominal maximum size of 5 mm, the fine aggregate was natural siliceous sand with grain size ranging from 0.15 to 0.5 mm and CEM I 42.5N of the Suez Company – Suez factory. The materials also include quartz powder used as a filler form with Blain fineness of 470 m<sup>2</sup>/Kg, and a specific gravity of 2.63, Clean drinking fresh water free from impurities, and chemical admixture. Silica fume was used as addition for the cement to produce workable concrete with high cubic compressive strength. Super-plasticizer was used to produce self-leveling concrete with only the water necessary for the hydration of the cement. Deformed high tensile steel of elastic strength of 420 MPa and ultimate strength of 630 MPa was used for all tested columns

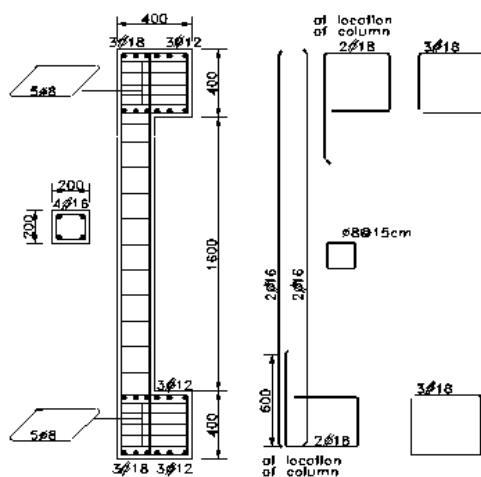
### Fabrication Of Test Columns And Test Setup

According to Khattab. E et al <sup>[5]</sup>, the design cube compressive strength of the concrete was 141 MPa after 90 days. The concrete mix consists of 800 Kg/m<sup>3</sup> cement content, 154 Kg/m<sup>3</sup> water, 318.8 kg/m<sup>3</sup> quartz powder, 318.8 kg/m<sup>3</sup> siliceous sand, 637.5 kg/m<sup>3</sup> crushed dolomite, 160 kg/m<sup>3</sup> silica fume and finally 32 kg/m<sup>3</sup> super plasticizer. The fresh concrete had a 550 mm slump flow; it was closed to self-compacting concrete. Two wood forms were prepared for casting the concrete. Concrete was cast in the material laboratory of Housing and Building National Research Center at 25° C temperature. The specimens were moist cured after de-molding and have a stem curing for 2 days.

The longitudinal steel of the column consisted of four rebars of 16 mm nominal diameter arranged symmetrically in the cross section. Figure (1) shows reinforcement details of the test specimens. Steel reinforcement percentage was 2% which is a typical practical value for eccentrically loaded columns. The transverse reinforcement of columns comprised 8 mm nominal diameter peripheral hoops. The hoops were spaced 190 mm with a volumetric ratio of 0.424%. The hoops had 135-bends extending 60 mm into concrete core. The core size was measured

from the center of the peripheral hoop. It was kept constant at 160x160 mm.

To avoid the premature failure, the corbels were heavily reinforced with 18 mm nominal diameter deformed rebars in the shape of vertical reinforcement in direction of bending moment. At 35 mm spacing, transverse ties of 8 mm diameter were arranged to sustain splitting forces. Another precaution to avoid premature failure, was concentrating transverse reinforcement of column at its ends in order to give enough confinement to overcome stress concentration at those ends.



All dimensions are in (mm)

Figure (1) Reinforcement Details of The Test Specimens

#### Test Setup And Instrumentation

The specimens were tested up to failure using AMSLER compression testing machine of 5000 kN capacity. The testing machine consists of lower moving piston which moves on a spherical head covered by a plate so that the applied load is always passing through the center of the sphere, and perpendicular to the column's cross section whenever the eccentricity is applied. On the other hand, the upper plate is moving around fixed sphere. A 5000 kN load cell was used to calibrate the machine. The load was measured through a pressure sensor which was fed-in addition to other test data-into a data acquisition system. The voltage excitations were read, transformed, and stored as microstrains, forces, and displacements by means of a virtual instant computer program runs under "LABVIEW" software. The rate of collecting data was one scan per second. The load eccentricity was achieved using bearing plates of 150 x 150 mm<sup>2</sup>, which is a relatively small area to simulate a concentrated eccentric column load. The specimen was placed on a lower bearing plate and the load was applied through an upper one. In addition, the bearing plates contain a semispherical mass to

allow for specimen rotation. Thus, the aforementioned considerations led the specimen to be pin-ended one. The machine heads ensured that the load eccentricity was maintained in all stages of loading. Figure (2) illustrate the details of the test setup and the used instrumentation. Axial displacement of the column was measured using linear variable distance transducers, (LVDT) with length of 500 mm. The LVDT,s were attached to the sides of RC columns using 3mm fisher bolts. One LVDT with length of 100 mm was attached to record the horizontal displacement of the column.

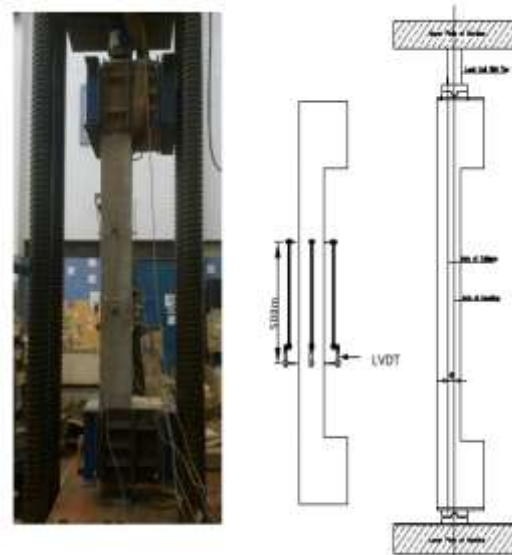


Figure (2) Test Setup and Instrumentation of The Specimens

#### IV. TEST RESULTS

All test results are summarized in this section, the load-longitudinal strain relationships, recorded at both of the extreme compression apex and the extreme tension apex. The maximum load capacity. The decrease in load carrying capacity compared to the control specimen. The maximum longitudinal concrete strain corresponding to the failure load.

Specimen (C1) is a column specimen subjected to axial loading. Figure (4) shows the load-longitudinal strain relationships, recorded at both of the extreme compression apex and the extreme tension apex. From the figure it is quite obvious that the hole section was under compression stresses. The maximum load capacity of the specimen was 3105 kn followed by an explosive failure at the middle third zone accompanied by a dramatic loss of load carrying capacity. The maximum longitudinal compressive concrete strain corresponding to the failure load was 0.00317.

Specimen (C2) is column subjected to an eccentricity of 20 mm. ( $e/t = 0.10$ ). Figure (5)

shows the load-longitudinal strain relationships, recorded at both of the extreme compression apex and the extreme tension apex. From the figure it is quite obvious that the hole section was under compression stresses. The maximum load capacity of the specimen was 2535 kn. The decrease in load carrying capacity compared to specimen (C1) was 18 %. The maximum longitudinal compressive concrete strain corresponding to the failure load was 0.00252.

Specimen (C3) is column subjected to an eccentricity of 40 mm. ( $e/t = 0.20$ ). Figure (6) shows the load-longitudinal strain relationships, recorded at both of the extreme compression apex and the extreme tension apex. The specimen had reached an ultimate load of 1768 kn. The decrease in load carrying capacity compared to specimen (C1) was 43 %. The maximum longitudinal compressive concrete strain corresponding to the failure load was 0.00246. The maximum load exerted a longitudinal tensile strain of 0.000748 for tension surface.

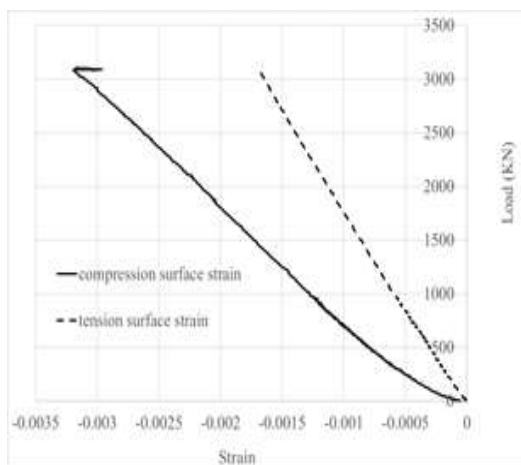


Figure (4): the load-longitudinal strain relationships of specimen (C1)

Specimen (C4) is column subjected to an eccentricity of 100 mm. ( $e/t = 0.50$ ). Figure (7) shows the load-longitudinal strain relationships, recorded at both of the extreme compression apex and the extreme tension apex. The specimen had reached an ultimate load of 339 kn. The decrease in load carrying capacity compared to specimen (C1) was 89 %. The maximum longitudinal compressive concrete strain corresponding to the failure load was 0.00141. The maximum load exerted a longitudinal tensile strain of 0.0211 for tension surface.

Specimen (C5) is column subjected to an eccentricity of 200 mm. ( $e/t = 1.00$ ). Figure (8) shows the load-longitudinal strain relationships, recorded at both of the extreme compression apex and the extreme tension apex. From the figure it is quite obvious that the hole section was under tension stresses. The specimen had reached an ultimate load of 148 kn. The decrease in load carrying capacity compared to specimen (C1) was 95 %. The maximum load exerted a longitudinal tensile strain of 0.0236 for tension surface.

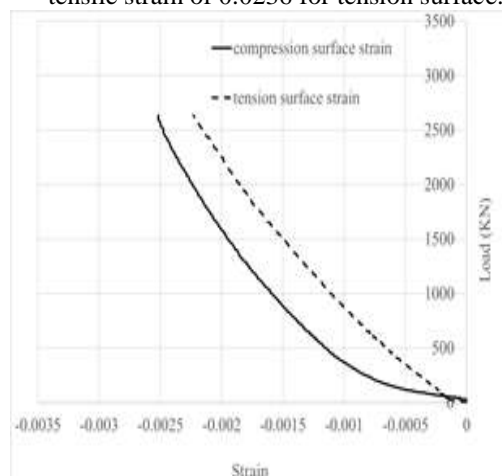


Figure (5): the load-longitudinal strain relationships of specimen (C2)

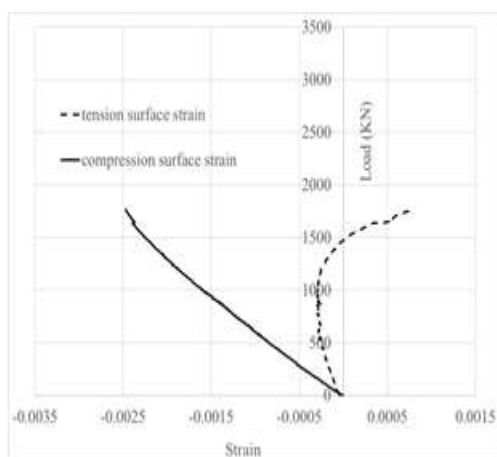


Figure (6): the load-longitudinal strain relationships of specimen (C3)

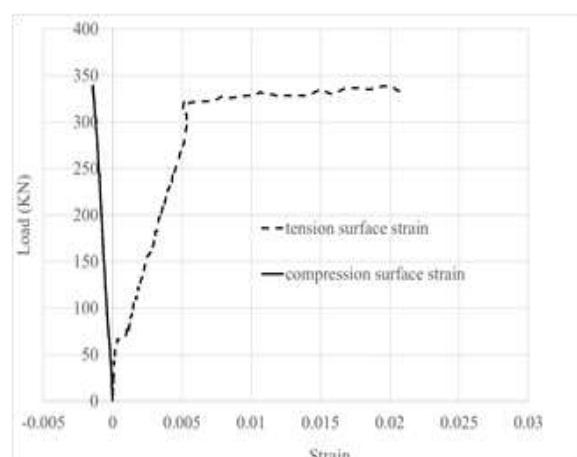


Figure (7): the load-longitudinal strain relationships of specimen (C4)

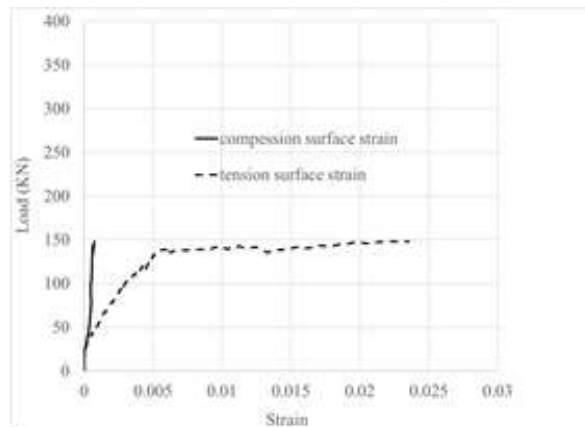


Figure (8): the load-longitudinal strain relationships of specimen (C5)

### Failure Modes Of Columns

Failure Modes of columns were observed and recorded. The failure mode of column C1 was severely explosive brittle compression failure, occurring at the extreme compression apex and accompanied by spalling of large portions of concrete cover and mild buckling of compression reinforcement rebar at the extreme compression apex between two successive mid height ties. The failure was sudden and was accompanied by a severe loss of strength. The failure mode of column C2 was compression brittle failure starting at the middle third of column height by spalling of small portions of concrete cover and buckling of

longitudinal compression steel rebar. The failure was less brittle than that of C1 specimen. The failure mode of column C3 was bending failure with low degree of brittleness since the load dropped gradually when the concrete cover spalled off. Some hair tensile cracks were observed in the tension sides. The failure occurred at the compression zone accompanied by spalling of small portions of concrete cover. The failure mode of columns C4 & C5 was bending failure. It started by horizontal cracks in the mid height of column followed by crushing of concrete at the extreme compression apex.



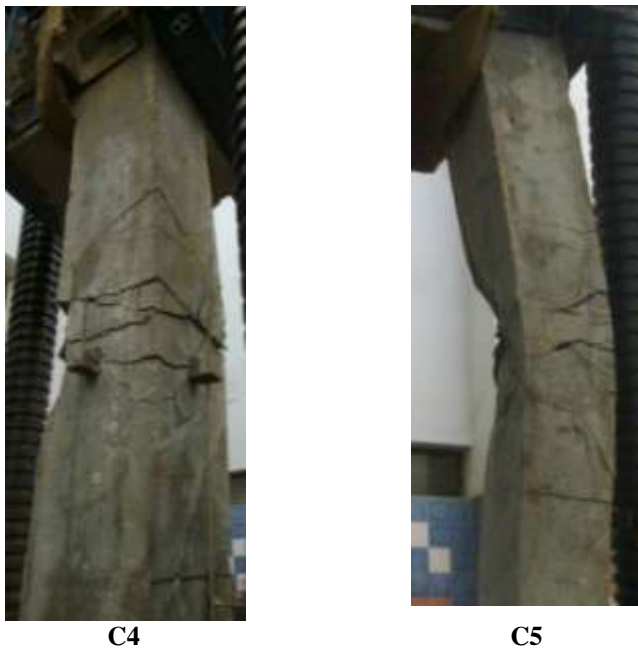
C1



C2



C3



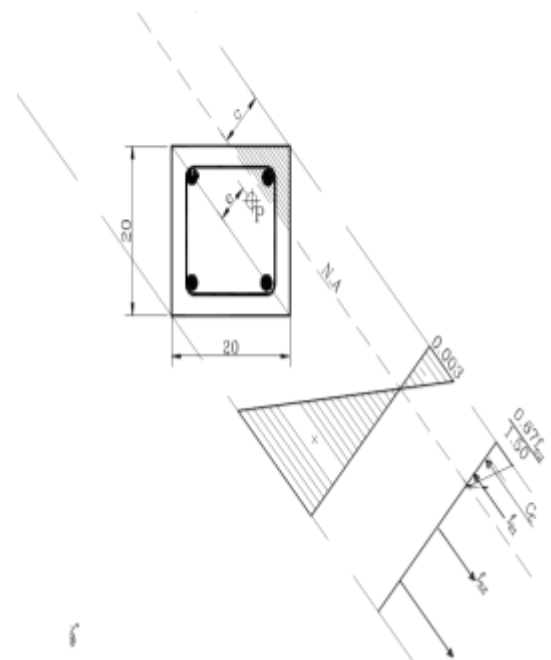
C4

C5

Figure (3) Failure Modes of Columns

**Experimental Verification with Code provisions**

The experimental ultimate strength ( $P_{exp}$ ) is compared with the values predicted by the Egyptian Code ECP 203-2007 (PECP). The theoretical loads were predicted as shown in Figure (4). As the section is subjected to biaxial bending and compressive axial force, it will be assumed that concrete young's modulus  $E_c$  is still constant up to ultimate load, this assumption is suitable for UHSC mixes Khattab. E et al [4]. The calculation of the values of ( $P_{ECP}$ ) was done by assuming the position of neutral axes and applying the equilibrium and compatibility equations for the different cases of reinforcement and compressive strength. Table (2) shows the experimental and predicted values for axial force for the different cases of compressive strength and reinforcement. It may be said that ECP provisions give a reasonable conservative estimate for ultimate load carrying capacity of the UHCS tested columns. The ratios of experimental-to-predicted values by the ECP vary from 3.41 to 1.45.



$$* P_{ECP} = C_c + f_{s1} + f_{s2} + f_{s3}$$

Fig.(4) Calculation of Values of ( $P_{ECP}$ )

**Table 2: Experimental and Predicted values for axial forces**

Column mm	e (mm.)	e/t	P <sub>ECP</sub> (KN)	P <sub>exp</sub> (KN)	P <sub>ECP</sub> /P <sub>exp</sub>
C2	20	0.1	742	2535	3.41
C3	40	0.2	589	1768	3.00
C4	100	0.5	198	339	1.71
C5	200	1.0	102	148	1.45

### V. CONCLUSIONS

From the analysis and discussion of the test results obtained from this research, the following conclusions can be drawn.

- 1- The eccentricity has a significant effect on the structural performance of biaxially loaded slender columns.
- 2- For UHSC columns by changing the eccentricity from (e/t = 0) to (e/t = 0.2), the ultimate load capacity was reducing by 43 % while by changing the eccentricity from (e/t = 0) to (e/t = 1), the ultimate load capacity was reducing by 95 %
- 3- The failure of ultra high strength concrete (UHSC) slender columns with no or low ratio of eccentricity occurred in a brittle Failure Mode while the failure mode of columns with high ratio of eccentricity was bending failure with low degree of brittleness.
- 4- The brittleness and less lateral strain of UHSC decrease the deformability of the biaxially loaded columns.
- 5- The provisions of the Egyptian Code for reinforced concrete (ECP203-2007) provided a reasonable conservative estimate for the

capacity of UHSC slender columns subjected to biaxial bending.

### REFERENCES

- [1]. Claeson, C., and Gylltoft, K., (1998), "Slender High-Strength Concrete Columns Subjected to Eccentric Loading", *Journal of Structural Engineering*, ASCE, Vol. 124, No. 3, March, 1998, pp.223-240.
- [2]. Ghoneim, M., (2002), "Strength of Slender High Strength Concrete Columns Under Eccentric Compression Loads", *Journal of Engineering and Applied Science*, Faculty of Engineering, Cairo University, Vol 49, No 6, December 2002, pp. 1157-1176.
- [3]. Tarek, M. E., "Behavior of Normal and High Strength Concrete Slender Columns Under Biaxial Bending", Ph.D. thesis, Cairo university, (2010).
- [4]. Khattab. E.A.A., El-Karmoty. H. Z., Abdelrahman.A. A., El-Dieb, AS., Bahnasawy. H. H., Okba S. H., "Theoretical and Experimental Study of Ultra High-Strength Reinforced Concrete Columns Under Axial Loads" *International Conference on Innovative Materials*, December 2016, Cairo, Egypt.
- [5]. Khattab. E.A.A., El-Karmoty. H. Z., Abdelrahman.A. A., El-Dieb, AS., Bahnasawy. H. H., Okba S. H., "Mix Proportions and Properties of Ultra High Strength Concrete Produced Using Local Materials" *HBRC Journal*, Vol. 6, No. 3, Dec 2010, pp. 9-19.

Dr. Ghada D. Abd-Elhamid "Structural Behaviour Of Ultra High Strength Concrete Columns Under Biaxial Loading " *International Journal of Engineering Research and Applications (IJERA)* , vol. 8, no.10, 2018, pp 44-50